Alzheimer-like pathology in the parietal cortex and hippocampus of aged donkeys

Article

Alzheimer-like pathology in the parietal cortex and hippocampus of aged donkeys

Alexandra J Malbon[a†*], Lorena Sordo[a†], Liam A Wilson[a], Danièlle Gunn-Moore[a], Georgios Paraschou[b], Neil Macintyre[a], Tobias Schwarz[a], Bruce McGorum[a], and Caroline Hahn[a]

[a] The Royal (Dick) School of Veterinary Studies and The Roslin Institute, University of Edinburgh, Easter Bush Campus, Midlothian, EH25 9RG, United Kingdom; AJM – amalbon@ed.ac.uk; LS – Lorena.sordo@ed.ac.uk; LAW – liam.wilson@ed.ac.uk; DGM – Danielle.gunn-moore@ed.ac.uk; NM – ne17mac@gmail.com; TS – tobias.schwarz@ed.ac.uk; BM – bruce.mcgorum@ed.ac.uk; CH – Caroline.hahn@ed.ac.uk

[b] Department of Pathobiology and Population Sciences, Royal Veterinary College, Hatfield, Hertfordshire, AL9 7TA, United Kingdom; GP - gparaschou@rvc.ac.uk

† These authors contributed equally.

* Correspondence

Abstract: Neurodegenerative disorders are gaining ever more importance in ageing populations of animals and people. Altered insulin signaling and type II diabetes have been linked to the development of Alzheimer's disease (AD) in humans and AD-like neurodegeneration in other long-lived animals. Donkeys are unusual amongst domestic species for their exceptional longevity and are additionally predisposed to abnormalities of insulin metabolism similar to those found in humans. In this study, the parietal lobe and hippocampus of 13 aged (> 30 years) and two younger control donkeys were evaluated immunohistologically for the presence, distribution, and frequency of neurofibrillary tangles (NFT) and amyloid plaques (AP); the characteristic lesions of AD. AP were in parietal cortices of nine donkeys, with a predilection for deep sulci, and NFT-like structures were observed in seven donkeys, primarily within cortical areas. No changes were observed in the control donkeys. This represents the first identification of both AP and NFT in equids and is a stimulus for future work assessing their metabolic status in parallel.

Highlights:

- AP and NFT-like structures were identified in equid brains for the first time
- These changes were only observed in brains from the aged donkey group
- This study opens the door to comparing human and asinine disorders of metabolism

Keywords: Donkey, Neurodegeneration, Alzheimer's, Neurofibrillary Tangles, Amyloid Plaques.

1. Introduction

Ageing is associated with a number of recognised degenerative changes in the human brain, some of which are accompanied by clinical signs of cognitive dysfunction. The most prevalent degenerative diseases are broadly grouped as dementia, with Alzheimer's disease (AD) the most frequent form (Kovacs, 2015). The two major neuropathologies seen in people affected with AD are the formation of extracellular amyloid-β plaques (AP) and the presence of intracellular neurofibrillary tangles (NFT) composed of a hyperphosphorylated form of the protein tau (Perl, 2010).

Despite its growing importance at an individual and economic level, the experimental study of AD is limited by the availability of valid spontaneous correlates. Mouse models rely on transgenic strains which can only partially mimic natural disease (King, 2018). Some non-human primates develop

Deleted: – a preliminary investigation

Deleted: together

the same pathological lesions as seen in AD (Darusman et al., 2014; Forny-Germano et al., 2014; Lyra e Silva et al., 2019; Oikawa et al., 2010), but in addition to ethical considerations, there are high financial costs in studying a sporadically occurring disease.

Recent studies have shown that aged individuals of other species naturally develop similar changes within their brains, including dogs (Cummings et al., 1996; Youssef et al., 2016), ruminants (sheep, goats, and cattle (Braak et al., 1994; Costassa et al., 2016; Reid et al., 2017)), cats (domestic cats (Chambers et al., 2015; Gunn-Moore et al., 2006; Head et al., 2005), leopards (Chambers et al., 2012), cheetahs (Serizawa et al., 2012)) and horses (Capucchio et al., 2010). However, not all species develop both AP and NFT lesions (Youssef et al., 2016).

Age-related changes in the brains of equids have been mainly studied in horses. These changes include the deposition of lipofuscin (Capucchio et al., 2010; Jahns et al., 2006) and hemosiderin (Jahns et al., 2006; Saunders, 1953) as well as the presence of calcium deposits (Capucchio et al., 2010; Hurst, 1934; Jahns et al., 2006), pre-amyloid plaques (silver stain positive but negative by Congo red and immunohistology, discussed in Capucchio et al. 2010) and neuronal swelling (Capucchio et al., 2010) . To date, NFT have not been identified in equids (Capucchio et al., 2010).

To the authors' knowledge, no studies have examined the brains of aged donkeys.

2. Materials and Methods

2.1 Samples, collection, and processing

This study included 13 elderly donkeys from southern England (three mares and ten geldings) aged between 30 and 44 years old, and two young control donkeys (geldings aged 8 and 9 years old). All donkeys were housed in loose barns over winter (approx. mid October to mid April) and strip-grazed outdoors over summer with indoor access maintained. They were humanely euthanised on purely clinical grounds, using 20 ml intravenous Somnulose (Dechra; Cinchocaine Hydrochloride, Quinalbarbitone Sodium); supplemental Table 1 provides the signalment and relevant findings for each animal. The elderly animals were euthanased owing mostly to age-related diseases, whilst both control donkeys were affected by sarcoids (a common equine dermal neoplasm which can severely impact quality of life). Post-mortem examination and sample collection was performed with full owner consent, within 2 - 30 hours of euthanasia.

Brains were fixed in 10% buffered formalin for at least one week before undergoing serial transverse sectioning. Samples from the parietal cortex and hippocampus were routinely processed into paraffin wax before mounting consecutive sections of 6 µm onto positively charged slides.

2.2 Immunohistology and special staining

For each case, immunohistology (IH) was performed on one section each of parietal cortex and hippocampus by immunolabelling with mouse and rabbit monoclonal anti-beta amyloid antibodies (4G8, [BioLegend, San Diego CA, US] and mOC64, [Abcam, Cambridge, UK] respectively), plus a mouse monoclonal anti-hyperphosphorylated tau (AT8; Thermo Fisher Scientific, Waltham MA, US). 4G8 targets amino acid residues 17-24 of ß amyloid. The epitope lies within amino acids 18-22 of β amyloid (VFFAE). 4G8 β-amyloid antibody reacts to abnormally processed isoforms, as well as precursor forms. mOC64 recognizes monomeric, oligomeric and fibrillar forms of β-amyloid 1-42 peptide, the epitope lies within amino acids 3-6.

4G8 is commonly used in human diagnostics; however owing to a predicted aa mismatch between the human and asinine sequence at position 19 (human reference XP_003364220.1) and no mismatch at 3-6, both antibodies were used in order to compare their performance. AT8 targets tau phosphorylated at Ser202 and Thr205. As this demonstrates the presence of tau-containing neurons but not their ultrastructure, positive cells are referred to from now on as NFT-like structures. Pre-treatment for antigen retrieval was performed in 98% formic acid for 6 hours for the anti-amyloid antibodies, and heat incubation at 110 °C in 0.01M sodium citrate buffer (pH 6.0) for 5 minutes for AT8. For all antibodies, slides were incubated in Dako REAL peroxidase blocking solution (Agilent Technologies, Stockport, UK) for 10 min to block endogenous peroxidase activity. Three times 2 min washes in Tris

Deleted: under

Deleted: ß

Deleted: ß

buffered saline plus tween 20 pH 7.6 were performed between each step. Primary antibodies were incubated overnight at room temperature (4G8 at 1:1,500; mOC64 at 1:12,000; AT8 at 1:200) and bound antibody was detected using Dako EnVision Mouse/Rabbit HRP for 40 min (Agilent Technologies). Antibody binding was visualised using 3, 3'-diaminobenzidine substrate for 10 min (DAB; Sigma-Aldrich, St. Louis MO, US) followed by 20 s counterstaining with Harris Haematoxylin (Sigma-Aldrich).

Following examination of these sections, representative sections with the most extensive immunostaining for AP (case 8) underwent immunohistology for the astrocyte marker glial fibrillary acidophilic protein (GFAP [rabbit polyclonal, Dako]) and the microglial marker Iba1 (rabbit polyclonal, Fujifilm Wako Chemicals, Neuss, Germany). GFAP was used at 1:400, incubated for 30 in at room temperature following pre-treatment of 30 min in Dako pre-diluted Proteinase K at 37 °C and Dako EnVision anti-rabbit detection. Iba1 was used at 1:500 for 30 min at room temperature, following pre-treatment in citrate buffer as above with Dako EnVision anti-rabbit detection.

Congo red staining was also performed on a subset of IH amyloid positive cases (8, 10, and 12).

2.3 Digital image analysis and scoring

Glass slides were first digitised using a Hamamatsu Nanozoomer whole slide scanner with a single layer scan at an up to 40x magnification then imported into QuPath (Bankhead et al., 2017), an open source image analysis software. Before image analysis began, the stain vectors for each slide were separately estimated using the modal values of QuPath's automatic vector estimation function to provide greater inter-slide consistency. Regions of interest (ROI) were delineated as white matter, sulci and gyri on the sections of parietal lobe. The sulci ROI included all grey matter up to the level of the most superficial white matter, whilst the gyri incorporated the remnant overlying grey matter, as previously described (Gentleman et al., 1992). The hippocampus was divided into the dentate gyrus, Cornu Ammonis (CA)4, CA3, CA2 and CA1 (Schröder, Moser and Huggenberger, 2020). These ROI avoided any large, overt artefactual changes including tissue folding or non-specific stain deposition, and are shown below in Figure 1.

The positive cell detection function was trained separately for 4G8, mOC64, and AT8 adapted from previously published methods (Wilson et al., 2021). Walker et al., 2017). This resulted in use of the following parameters in all three immunolabels: optical density sum detection image, pixel size 0.5µm, background radius 8µm, median filter radius 0µm, sigma 2µm, maximum area 0µm (equivalent to infinite), detection threshold 0.2, maximum background intensity 4 and score compartment of cell: DAB optical density mean. The minimum area varied from 26.45µm2 for the AT8 sections, to 100µm2 for the 4G8 and mOC64. The cell expansion was 1µm for the AT8 sections, 25µm for the 4G8 and 1.5µm for the mOC64 whilst the score threshold was 0.65, 0.3 and 0.2 respectively.

This methodology was then used on each section, with measurements exported to Microsoft Excel. These measurements included a count of the total area of the anatomical ROIs for each section. For the AT8 sections, the total count of AT8 positive neurons in each area was measured and used to calculate the number of positive detections per cm^2. For 4G8 and mOC64, area density was instead used.

To simplify data visualization, thresholds were determined for each stain which corresponded to -, +, ++, and +++ scores. These were chosen by trialling iterations of histogram data bins to establish which allowed optimum segregation of the data.

For 4G8, these were set at 0.06 % and 0.12 %, with 0.006 % and 0.012 % for mOC64 and 0.05 and 0.5 cells/cm^2 for AT8.

Formatted: Justified

Deleted: t

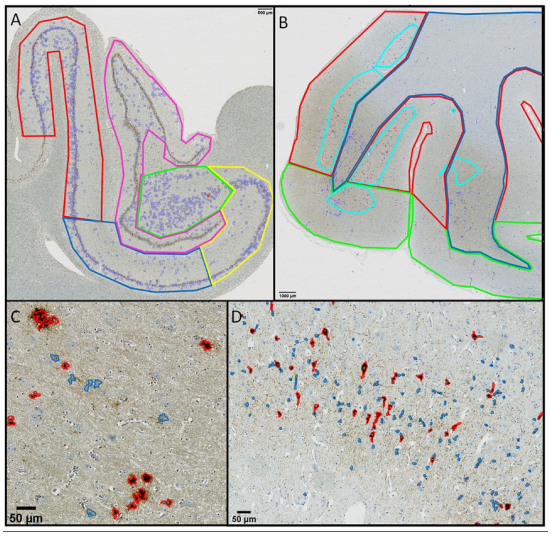

Figure 1: Images captured from QuPath. (A) Delineation of hippocampal anatomical regions of interest (ROIs), case 9 hippocampal region immunolabelled with 4G8. The purple ROI highlights the dentate gyrus, the green Cornu Ammonis (CA)4, the yellow CA3, the blue CA2 and the red CA1. Note that the larger detections in this area equate to the 25µm expansion of each positive detection, as detailed in the methods section. [B] Delineation of parietal lobe anatomical ROIs, case 8 parietal lobe immunolabelled with mOC64. The blue ROI highlights the white matter, the red ROIs highlight the various sulci, the green highlight the gyri and the cyan areas highlight areas of true positive cell detections. [C] 4G8 positively immunolabelled amyloid plaques with positive detections highlighted by a red outline, case 9 parietal lobe immunolabelled with mOC64. [D] AT8 positive neurofibrillary tangle-like structures with positive detections highlighted by a red outline, case 13 parietal lobe immunolabelled with AT8.

Deleted: s

2.4 Statistical analysis

The statistical package GraphPad Prism was used for all statistical comparisons and graphical representations. Results for each region and antibody were first assessed for normality. As this gave variable results non-parametric tests were used for all. A Spearman's rank correlation was used for correlation between the two AP antibodies, between 4G8 and AT8, and between each antibody and age. A one-way ANOVA was applied to regions of each section, with Wilcoxon matched pairs signed rank test used to identify significant pairwise comparisons. A probability of 0.05 was used as the cut off for all analyses, performed two-tailed.

3. Results

3.1 Amyloid plaques (AP)

All observed plaques corresponded to those described in human literature as diffuse, with no entrapment of dying neurons or associated gliosis. The latter was confirmed by GFAP and Iba-1 staining (exemplified in Supplemental Figure 1). There was a mild discrepancy in immunolabelling between the two antibodies, with more intense and slightly more widespread positive immunolabelling observed with 4G8 than mOC64. This is reflected in the differing thresholds set using QuPath data, and the increased number of low scoring cases with 4G8 (Table 1). However, a Spearman's rank correlation between the two antibodies for the parietal cortex indicated correlation at $p < 0.0001$ indicating that this difference was likely of sensitivity rather than any inherent difference in target antigen. The 4G8 stain

also diffusely labelled neuronal cytoplasm with granular positivity. This affected all neurons with no discernible difference based on size or anatomical layer. AP were detected by both antibodies in the parietal cortex of seven of the 13 aged donkeys. There was a very low level of detection in a further two donkeys in 4G8 only. Within the hippocampus itself (i.e. excluding the cortical areas present in the section at the level of the hippocampus) there was very low level AP plaque load detected in almost all using 4G8 but not mOC64. None were observed in the young donkeys. The grey matter was predominantly affected, though not exclusively, with a predilection for sulcal depths. Sulci were significantly more affected than white matter ($p < 0.01$) but not than gyri (0.0742). There was no positive staining outwith plaque formations, e.g. of vessel walls.

Congo red staining of the three donkeys with the highest AP load was negative in the AP as well as in other structures e.g. vessel walls (exemplified in Supplemental Figure 1).

Table 1: Summary of immunohistological findings by individual animal and anatomical region.

		AP				NFT-like structures	
Donkey	Age (yrs)	4G8		mOC64		AT8	
		P	H	P	H	P	H
1	8	-	-	-	-	-	-
2	9	-	-	-	-	-	-
3	30	+	+	++	-	-	-
4	31	-	-	-	-	-	-
5	31	+	+	-	-	-	-
6	31	+	+	+	-	-	-
7	31	+++	+	+++	-	+	++
8	32	+	+	++	-	++	-
9	33	+	+	-	-	-	-
10	33	+++	+	++	-	+	-
11	34	-	+	-	-	-	-
12	34	++	+	+	-	+	-
13	34	++	+	+++	-	+++	++
14	37	-	+	-	-	++	-
15	44	-	+	-	-	+	-

AP – amyloid plaques; NFT – neurofibrillary tangles; P – parietal cortex; H – hippocampus.

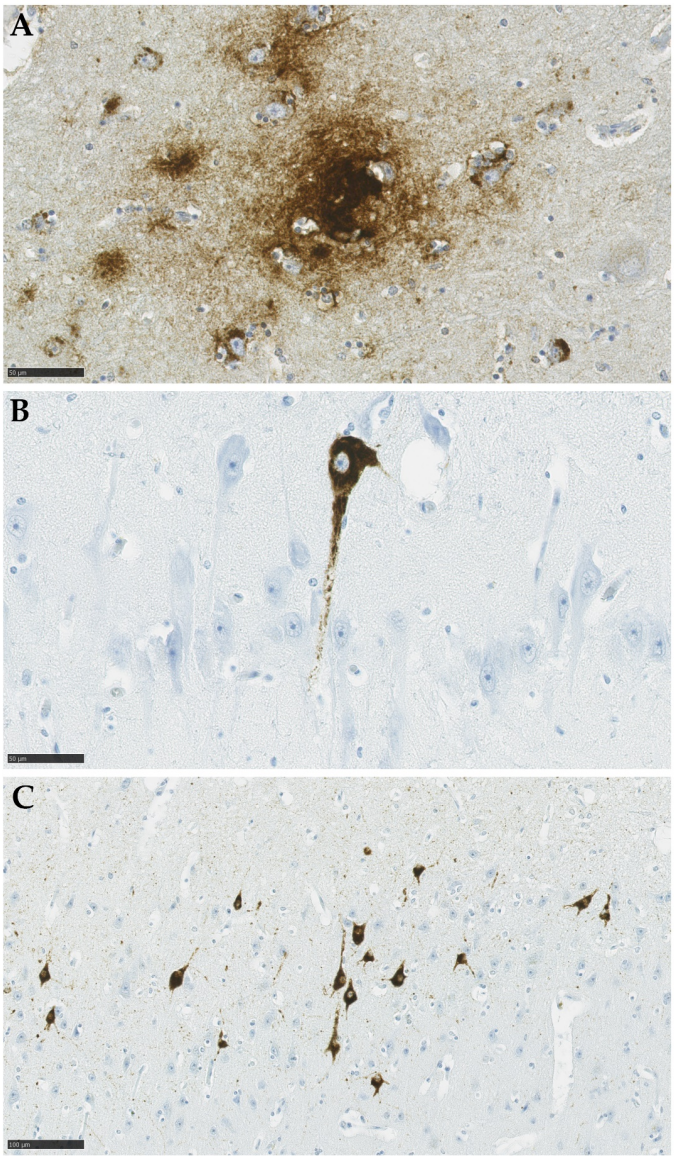

Figure 2: Representative images of amyloid plaques (AP) and neurofibrillary tangle (NFT)-like structures immunolabelled by 4G8 and AT8, respectively. (A) AP in the cortical grey matter of donkey 7 (31-year old gelding)– scale bar 50µm; (B) An isolated NFT-like structure from hippocampal region CA1 of donkey 13 (34-year old gelding)– scale bar 50µm; (C) More frequent NFT-like structures observed in the parietal cortex of donkey 13 – scale bar 100µm.

Deleted: s

Deleted: the

Commented [AM1]: Higher power as requested

Deleted: us

Deleted: 2

3.2 Neurofibrillary tangle-like structuress (NFT)

The NFT were observed in the parietal cortex of seven aged donkeys (Table 1). They predominantly, though not exclusively, affected pyramidal cells; equivalent to mainly cortical layers III and V. Two of these donkeys also showing immunolabelling in the hippocampus. Positive cells here consisted of very rare individual cells in CA1 (both cases) and CA4 (one case). Cortical neurons at the level of the hippocampus were far more frequently affected than those of the hippocampus itself (data not shown). Neither of the young donkeys exhibited NFT. Owing to the limited regions available to assess, no staging of the type used in humans (e.g. Braak and Braak, 1991) was attempted.

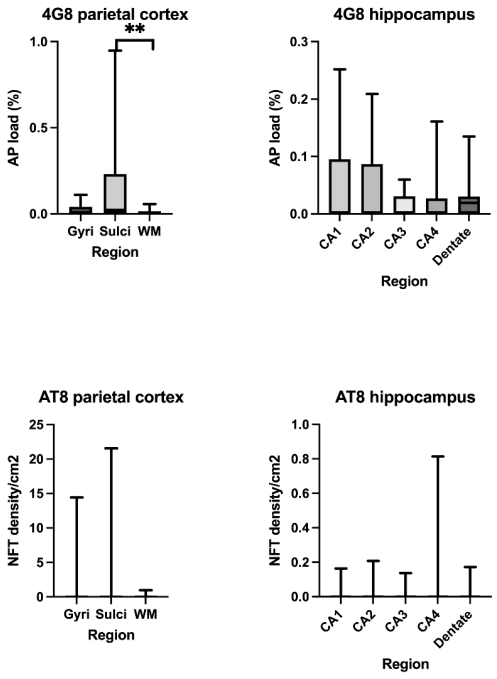

Figure 3: Bar charts showing minimum to maximum immunohistological scores, demonstrating distribution of amyloid plaques (AP) and neurofibrillary tangles (NFT) by region in both the parietal cortex and the hippocampus of all donkeys. WM – white matter; CA – Cornu Ammonis; ** - significance level of $p < 0.01$.

3.3 Correlation

Five of the seven cases positive for NFT-like structures also exhibited AP in the same section. However, from the results so far, there is no statistically significant association between the presence of AP and NFT in an individual (4G8 vs AT8; $p = 0.5578$). There was also no spatial correlation visible on an observational basis when comparing consecutively stained slides. Overall, more AP than NFT were observed; see Table 1. Figures 4A and B, and G and H show good agreement between the two AP antibodies, with no associated hyperphosphorylated tau presence in C. Images D – F show NFT-like structures in the absence of AP whilst G - L demonstrate the presence of NFT and AP in the same region, based on consecutively stained sections (~6 µm apart).

Deleted: and were not restricted to any specific cortical depth, with

Deleted: t

Deleted: D and E, and G and H

Deleted: ,

Deleted: F, or I

Deleted: . Image L

Deleted: s

The two younger control donkeys had no detectable AP or NFT. Within the older animals, there was no statistically significant age correlation detected for either AP or NFT, though this may reflect the relatively low case numbers. This was performed for the anatomical regions overall as well as individually by location within (e.g. sulci). Table 1 summarises the findings by individual.

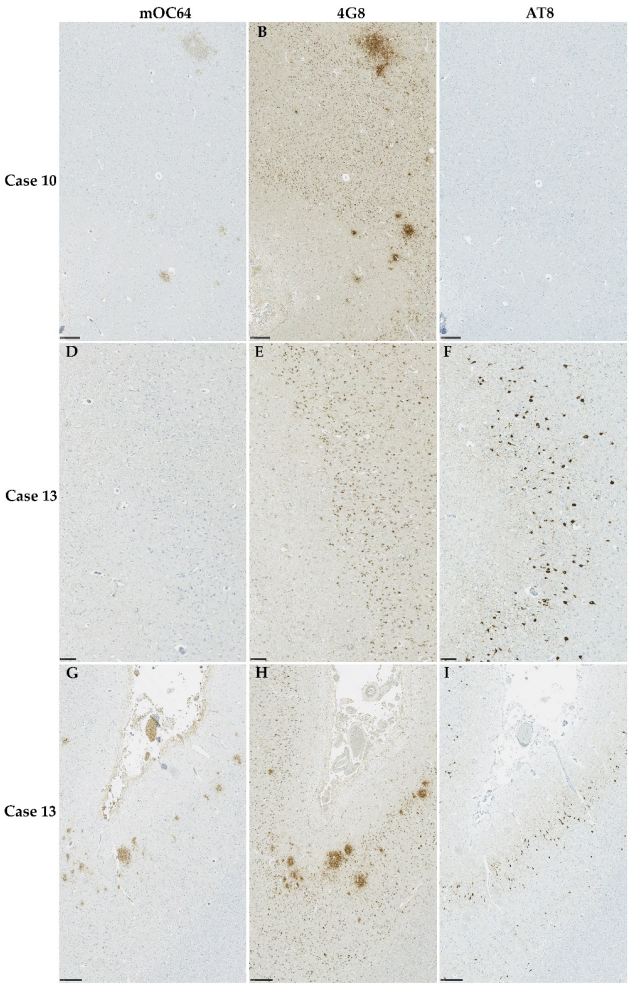

Figure 4: Spatial correlation between amyloid plaques (using the two immunolabels mOC64 and 4G8) and neurofibrillary tangles (using immunolabel AT8) in the parietal cortex of case 10 (33-year old gelding), and case 13 (34-year old gelding). Scale bars per row are of 250 µm, 100 µm, and 250µm respectively.

Deleted: ; 4G8

Deleted: mOC64

Deleted: .

Deleted: Rows 1-4 represent donkeys 9, 7, 10, and 13 respectively, columns 1-3 represent 4G8, mOC64, and AT8, respectively

4. Discussion

This is the first report of classical markers of AD-like neurodegeneration, i.e. AP and NFT, in the brains of aged equids, and specifically donkeys.

While the degenerative changes were only seen in the aged donkeys, not the young controls, it was not possible to further correlate the incidence or severity of degenerative changes – as indicated by AP and NFT – with increasing age, possibly due to small sample size or extraneous factors including genetics. The oldest animal (at 44 years of age, eight years older than the second oldest) in fact exhibited neither AP nor NFT-like structures in the examined regions, suggesting that the presence of these changes is not an inevitable ageing change. Similarly, more cases would be required to determine whether there is a trend for either AP or NFT to occur first and whether these are spatially linked. One donkey (case 13) appeared to show co-localisation; however, it cannot be excluded that this is incidental owing to the widespread presence of NFTs in this case. Braak staging (Braak and Braak, 1991) is generally the accepted method to assess the stage of disease in humans. This could not be performed with the limited regions available and as such future studies require comparison of disease progression between species. If sequential involvement is similar, hippocampal involvement would indicate stage III or IV out of VI.

As previous studies on ageing changes in brains of horses identified neither immunohistologically positive AP nor NFT, this may reflect a true species difference between horses and donkeys, or rather the older age of our cases, extending almost 20 years beyond the oldest animals in the equine studies (Capucchio et al., 2010; Jahns et al., 2006).

Numerous types of AP have been described but the two most frequently identified in AD are diffuse and dense core plaques (DeTure and Dickson, 2019). The AP identified in the present study are consistent with diffuse plaques (Kovacs, 2015; Thal et al., 2006), mirroring previous findings in cats and dogs (Gunn-Moore et al., 2006; Head et al., 2005, 2000; Kovacs, 2015). It is suspected that diffuse plaques may be precursors to dense core plaques; the latter more commonly associated with neuronal and microglial degenerative changes (Thal et al., 2006). Their effect in equids is currently unclear. Diffuse plaques are also known to be poorly immunoreactive, with varying sensitivity of different antibodies (Kovacs, 2015), reflected in the results of the present study. This may also explain the lack of immunoreactivity of the plaques observed in horse brains by Capucchio et al. (2010). Although the location of mOC64-positive deposits corresponded to those observed with the 4G8 antibody in any given individual, 4G8 staining (which also detects amyloid precursor protein) was observed more intensely and with a slightly wider distribution. As in humans, grey matter, and more specifically sulci, appears predisposed.

In humans, the distribution of NFT follows a set pattern as the disease progresses, allowing six stages to be recognised (Braak and Braak, 1991). Amyloid deposition can show more variability but also follows a pattern in humans and dogs (Braak and Braak, 1991; Head et al., 2000; Thal et al., 2006). We observed NFT in the parietal cortex more frequently than the hippocampus, with the latter never affected without the adjacent cortex. Evaluation of additional brain regions and many more donkeys of different ages will be required to determine if the same patterns apply in donkeys.

Although they are distinct features of AD, AP and NFT may precede clinical disease by decades (DeTure and Dickson, 2019). From a welfare perspective this study alerts the veterinary profession and those working with donkeys to the need to be watchful for clinical signs of cognitive decline. It is necessary to be able to assess the behaviour of these animals more accurately in order to determine any clinical significance and the potential impact on the animal's quality of life. A system for equine cognitive function testing has been developed (Roberts et al., 2017) and may be of potential benefit in the assessment of donkeys. However, its aim was to use the horse as a model in neurological disorders, specifically looking at stereotypical behaviours (Roberts et al., 2017), therefore adaptations or a novel donkey cognitive function system may be required to take into account species differences.

This study represents the preliminary stage of investigation into changes occurring in the ageing asinine brain, and suggests that donkeys may undergo degenerative changes similar to those occurring in humans. It is hypothesized that this neurodegeneration is a result not of ageing itself but more specifically of our post reproductive longevity (Gunn-Moore et al., 2018). Resistance to insulin, or

reduced insulin signaling, has been shown experimentally to increase lifespan in mice and this altered responsiveness in insulin signaling pathways appears to be part of a trade off in humans contributing to the long post fertility lifespan (PFLS) (Gunn-Moore et al., 2018). PFLS is not unique to humans (indeed certain cetaceans share this, as well as AD-like disease (Cohen, 2004; Gunn-Moore et al., 2018)) but its frequency in other mammals is debated and can be difficult to assess (Cohen, 2004; Ellis et al., 2018). There are no data available for PFLS in donkeys, which is an area for future study. Compared to other domestic mammals including dogs and cats, which are currently being investigated as models (Chambers et al., 2015; Gunn-Moore et al., 2006; Head et al., 2005; Tokuda et al., 2015; Youssef et al., 2016), donkeys are exceptionally long lived. The finding of shared neuropathological changes with humans opens the door to perhaps the most intriguing aspect; their shared susceptibility to metabolic dysfunctions. The triad of T2DM, obesity, and AD are intricately linked in humans (Gunn-Moore et al., 2018; Monte and Wands, 2008; Pugazhenthi et al., 2017), with insulin dysregulation one of the main common factors. Equids, in particular donkeys, are known to be prone to their own version of insulin resistance, in the form of equine metabolic syndrome (EMS) (Durham et al., 2019; Mendoza et al., 2019; Morgan et al., 2015). Donkeys could therefore be a potential animal model for AD, with both species gaining from any useful observations. EMS is often associated with obesity, which leads to reduced hepatic clearance of insulin and dysregulation of adipokines such as leptin and adiponectin (Durham et al., 2019). Donkeys are prone to hyperlipaemia, further enhanced in obesity, and have associated elevated leptin levels indicating alterations in lipid metabolism (Díez et al., 2012). Adiponectin is overall neuroprotective and is in contrast decreased with increasing adiposity in horses (Radin et al., 2009). Both leptin and adiponectin have been linked to the development of AD (McGuire and Ishii, 2016; Waragai et al., 2017), it could therefore be hypothesized that there is a link between this species' elevated leptin and the observed neurodegenerative changes.

An additional area of interest for further investigation is the link between iron levels, metabolic syndrome, and neurodegeneration. Ferritin levels have been linked to hyperinsulinaemia in horses (Kellon and Gustafson, 2019), whilst in humans altered iron homeostasis is known to occur in numerous forms of neurodegeneration (Ward et al., 2014; Wojtunik-Kulesza et al., 2019).

Unintentionally, by treating donkeys as we would the domestic horse, when they have evolved to survive arid conditions, the effect may in many ways have been similar to that of a western diet on humans (Mendoza et al., 2019). It is currently unclear to what extent the relatively sedentary lifestyle of most donkeys in high income countries influences their susceptibility (Durham et al., 2019), it is therefore planned to expand the next stage of this study to include material from working donkeys.
In further studies we would aim to broaden the depth and scope of our investigation into the neurodegenerative changes affecting donkeys, to include both morphological and functional perspectives. Crucially, we also aim to incorporate assessment of the asinine metabolic status, both to evaluate whether this links to any neurological changes and to learn more about how close the human parallels are.

5. Conclusions

While NFT and AP are classically associated with human AD, this study is the first to report similar protein changes in the brains of aged donkeys. Further investigation is required to better understand the extent of these parallels.

Deleted: these

Author Contributions: For research articles with several authors, a short paragraph specifying their individual contributions must be provided. The following statements should be used "Conceptualization, D.G.M., B.M., C.H., T.S.; methodology, D.G.M., L.S., A.M., N.M.; validation, D.G.M., L.S., A.M.; formal analysis, A.M., L.W., N.M.; investigation, D.G.M., L.S.; resources, D.G.M., L.S., C.H., G.P.; data curation, L.S.; writing—original draft preparation, A.M., L.S; writing—review and editing, D.G.M., B.M., N.M., C.H., L.W., G.P.; visualization, A.M., L.W.; supervision, D.G.M., A.M.; project administration, D.G.M.; funding acquisition, D.G.M., B.M.. All authors have read and agreed to the published version of the manuscript.", please turn to the CRediT taxonomy for the term explanation. Authorship must be limited to those who have contributed substantially to the work reported.

Funding: This research received no external funding.

Acknowledgments: This study was supported by the Fiona and Ian Russell Seed Corn Fund for Companion Animal Research. We gratefully acknowledge the expert technical assistance of the histology laboratory staff at Easter Bush. We are also grateful to Prof Colin Smith and his histology laboratory staff at the Centre for Clinical Brain Sciences for additional immunohistology.

Conflicts of Interest: The authors declare no conflict of interest.

Supplemental figure 1 caption: Immunohistology and special staining of the parietal cortex of donkey 7 (31 year old gelding). The same site in all is at the junction of cortical grey (left) and white matter (right).

References

Bankhead, P., Loughrey, M.B., Fernández, J.A., Dombrowski, Y., McArt, D.G., Dunne, P.D., McQuaid, S., Gray, R.T., Murray, L.J., Coleman, H.G., James, J.A., Salto-Tellez, M., Hamilton, P.W., 2017. QuPath: Open source software for digital pathology image analysis. Sci. Reports 2017 71 7, 1–7. https://doi.org/10.1038/s41598-017-17204-5

Braak, H., Braak, E., 1991. Neuropathological stageing of Alzheimer-related changes. Acta Neuropathol. 82, 239–259. https://doi.org/10.1109/ICINIS.2015.10

Braak, H., Braak, E., Strothjohann, M., 1994. Abnormally phosphorylated tau protein related to the formation of neurofibrillary tangles and neuropil threads in the cerebral cortex of sheep and goat. Neurosci. Lett. 171, 1–4. https://doi.org/10.1016/0304-3940(94)90589-4

Capucchio, M.T., Márquez, M., Pregel, P., Foradada, L., Bravo, M., Mattutino, G., Torre, C., Schiffer, D., Catalano, D., Valenza, F., Guarda, F., Pumarola, M., 2010. Parenchymal and Vascular Lesions in Ageing Equine Brains: Histological and Immunohistochemical Studies. J. Comp. Pathol. 142, 61–73. https://doi.org/10.1016/j.jcpa.2009.07.007

Chambers, J.K., Tokuda, T., Uchida, K., Ishii, R., Tatebe, H., Takahashi, E., Tomiyama, T., Une, Y., Nakayama, H., 2015. The domestic cat as a natural animal model of Alzheimer's disease. Acta Neuropathol. Commun. 3, 78. https://doi.org/10.1186/s40478-015-0258-3

Chambers, J.K., Uchida, K., Harada, T., Tsuboi, M., Sato, M., Kubo, M., Kawaguchi, H., Miyoshi, N., Tsujimoto, H., Nakayama, H.D., Chad, A., 2012. Neurofibrillary tangles and the deposition of a beta amyloid peptide with a novel N-terminal epitope in the brains of wild Tsushima leopard cats. PLoS One 7, e46452.

Cohen, A.A., 2004. Female post-reproductive lifespan: a general mammalian trait. Biol. Rev. 79, 733. https://doi.org/10.1017/S1464793103006432

Costassa, E.V., Fiorini, M., Zanusso, G., Peletto, S., Acutis, P., Baioni, E., Maurella, C., Tagliavini, F., Catania, M., Gallo, M., Lo Faro, M., Chieppa, M.N., Meloni, D., D'Angelo, A., Paciello, O., Ghidoni, R., Tonoli, E., Casalone, C., Corona, C., 2016. Characterization of amyloid-β Deposits in Bovine Brains. J. Alzheimer's Dis. 51, 875–887. https://doi.org/10.3233/JAD-151007

Cummings, B.J., Head, E., Afagh, A.J., Milgram, N.W., Cotman, C.W., 1996. Beta-amyloid accumulation correlates with cognitive dysfunction in the aged canine. Neurobiol. Learn. Mem. 66, 11–23.

Darusman, H.S., Sajuthi, D., Schapiro, S.J., Gjedde, A., Kalliokoski, O., Kristianingrum, Y.P., Handharyani, E., Hau, J., 2014. Amyloid beta 1-42 and phoshorylated tau threonin 231 in brains of aged cynomolgus monkeys (Macaca fascicularis). Front. Aging Neurosci. 6, 1–7. https://doi.org/10.3389/fnagi.2014.00313

DeTure, M.A., Dickson, D.W., 2019. The neuropathological diagnosis of Alzheimer's disease. Mol. Neurodegener. 14, 1–18. https://doi.org/10.1186/s13024-019-0333-5

Díez, E., López, I., Pérez, C., Pineda, C., Aguilera-Tejero, E., Dıéz, E., Lo´pezlo´pez, I., Pe´rezpe´rez, C., 2012. Plasma leptin concentration in donkeys. Vet. Q. 32, 13–16. https://doi.org/10.1080/01652176.2012.677867

Durham, A.E., Frank, N., McGowan, C.M., Menzies-Gow, N.J., Roelfsema, E., Vervuert, I., Feige, K., Fey, K., 2019. ECEIM consensus statement on equine metabolic syndrome. J. Vet. Intern. Med. https://doi.org/10.1111/jvim.15423

Ellis, S., Franks, D.W., Nattrass, S., Cant, M.A., Bradley, D.L., Giles, D., Balcomb, K.C., Croft, D.P., 2018. Postreproductive lifespans are rare in mammals. Ecol. Evol. 8, 2482–2494. https://doi.org/10.1002/ece3.3856

Forny-Germano, L., Lyra E Silva, N.M., Batista, A.F., Brito-Moreira, J., Gralle, M., Boehnke, S.E., Coe, B.C., Lablans, A., Marques, S.A., Martinez, A.M.B., Klein, W.L., Houzel, J.C., Ferreira, S.T., Munoz, D.P., De Felice, F.G., 2014. Alzheimer's disease-like pathology induced by amyloid-β oligomers in nonhuman primates. J. Neurosci. 34, 13629–13643. https://doi.org/10.1523/JNEUROSCI.1353-14.2014

Gentleman, S.M., Allsop, D., Bruton, C.J., Jagoe, R., Polak, J.M., Roberts, G.W., 1992. Quantitative differences in the deposition of βA4 protein in the sulci and gyri of frontal and temporal isocortex in Alzheimer's disease. Neurosci. Lett. 136, 27–30. https://doi.org/10.1016/0304-3940(92)90639-O

Gunn-Moore, D., Kaidanovich-Beilin, O., Gallego Iradi, M.C., Gunn-Moore, F., Lovestone, S., 2018. Alzheimer's disease in humans and other animals: A consequence of postreproductive life span and longevity rather than aging. Alzheimer's Dement. 14, 195–204. https://doi.org/10.1016/j.jalz.2017.08.014

Gunn-Moore, D.A., McVee, J., Bradshaw, J.M., Pearson, G.R., Head, E., Gunn-Moore, F.J., 2006. Ageing changes in cat brains demonstrated by β-amyloid and AT8-immunoreactive phosphorylated tau deposits. J. Feline Med. Surg. 8, 234–242. https://doi.org/10.1016/j.jfms.2006.01.003

Head, E., McCleary, R., Hahn, F.F., Milgram, N.W., Cotman, C.W., 2000. Region-specific age at onset of β-amyloid in dogs. Neurobiol. Aging 21, 89–96. https://doi.org/10.1016/S0197-4580(00)00093-2

Head, E., Moffat, K., Das, P., Sarsoza, F., Poon, W.W., Landsberg, G., Cotman, C.W., Murphy, M.P., 2005. β-Amyloid deposition and tau phosphorylation in clinically characterized aged cats. Neurobiol. Aging 26, 749–763. https://doi.org/10.1016/j.neurobiolaging.2004.06.015

Hurst, E.W., 1934. Calcification in the Brains of Equidae and of Bovidae. Am. J. Pathol. 10, 795-798.3.

Jahns, H., Callanan, J.J., McElroy, M.C., Sammin, D.J., Bassett, H.F., 2006. Age-related and non-age-related changes in 100 surveyed horse brains. Vet. Pathol. 43, 740–750. https://doi.org/10.1354/vp.43-5-740

Kellon, E.M., Gustafson, K.M., 2019. Possible dysmetabolic hyperferritinemia in hyperinsulinemic horses. Open Vet. J. 9, 287–293. https://doi.org/10.4314/ovj.v9i4.2

King, A., 2018. A model challenge. Nature 559, S13–S15. https://doi.org/10.1083/jcb.200411001

Kovacs, G.G., 2015. Neuropathology of Neurodegenerative Diseases. Cambridge University Press.

Lyra e Silva, N. de M., Gonçalves, R.A., Boehnke, S.E., Forny-Germano, L., Munoz, D.P., De Felice, F.G., 2019. Understanding the link between insulin resistance and Alzheimer's disease: Insights from animal models. Exp. Neurol. 316, 1–11. https://doi.org/10.1016/j.expneurol.2019.03.016

McGuire, M.J., Ishii, M., 2016. Leptin dysfunction and Alzheimer's disease: evidence from cellular, animal, and human studies. Cell Mol. Neurobiol. 36, 203–217. https://doi.org/10.1016/j.physbeh.2017.03.040

Mendoza, F.J., Toribio, R.E., Perez-Ecija, A., 2019. Metabolic and Endocrine Disorders in Donkeys. Vet. Clin. North Am. - Equine Pract. 35, 399–417. https://doi.org/10.1016/j.cveq.2019.07.001

Monte, S.M. de la, Wands, J.R., 2008. Alzheimer's Disease Is Type 3 Diabetes–Evidence Reviewed. J. Diabetes Sci. Technol. 2, 1101. https://doi.org/10.1177/193229680800200619

Morgan, R., Keen, J., McGowan, C., 2015. Equine Metabolic Syndrome. Vet. Rec. 173–179. https://doi.org/10.1002/9781119169239.ch36

Oikawa, N., Kimura, N., Yanagisawa, K., 2010. Alzheimer-type tau pathology in advanced aged nonhuman primate brains harboring substantial amyloid deposition. Brain Res. 1315, 137–149. https://doi.org/10.1016/j.brainres.2009.12.005

Perl, D.P., 2010. Neuropathology of Alzheimer's Disease 77, 32–42. https://doi.org/10.1002/msj.20157.Neuropathology

Pugazhenthi, S., Qin, L., Reddy, P.H., 2017. Common neurodegenerative pathways in obesity, diabetes, and Alzheimer's disease. Biochim. Biophys. Acta - Mol. Basis Dis. 1863, 1037–1045. https://doi.org/10.1016/j.bbadis.2016.04.017

Radin, M.J., Sharkey, L.C., Holycross, B.J., 2009. Adipokines: A review of biological and analytical principles and an update in dogs, cats, and horses. Vet. Clin. Pathol. 38, 136–156. https://doi.org/10.1111/j.1939-165X.2009.00133.x

Reid, S.J., Mckean, N.E., Henty, K., Portelius, E., Blennow, K., Rudiger, S.R., Bawden, C.S., Handley, R.R., Verma, P.J., Faull, R.L.M., Waldvogel, H.J., Zetterberg, H., Snell, R.G., 2017. Alzheimer's disease markers in the aged sheep (Ovis aries). Neurobiol. Aging 58, 112–119.

Roberts, K., Hemmings, A.J., McBride, S.D., Parker, M.O., 2017. Developing a 3-choice serial reaction time task for examining neural and cognitive function in an equine model. J. Neurosci. Methods 292, 45–52. https://doi.org/10.1016/j.jneumeth.2017.01.018

Saunders, L.Z., 1953. Cerebrovascular siderosis in horses. A. M. A. Arch. Pathol. 56, 637–642.

Schröder, H., Moser, N., Huggenberger, S., 2020. The Mouse Hippocampus, in: Neuroanatomy of the Mouse. Springer, Cham, pp. 267–288. https://doi.org/10.1007/978-3-030-19898-5_11

Serizawa, S., Chambers, J.K., Une, Y., 2012. Beta amyloid deposition and neurofibrillary tangles spontaneously occur in the brains of captive cheetahs (Acinonyx jubatus). Vet. Pathol. 49, 304–312.

Thal, D.R., Capetillo-Zarate, E., Del Tredici, K., Braak, H., 2006. The development of amyloid beta protein deposits in the aged brain. Sci. Aging Knowledge Environ. 2006, 52–54. https://doi.org/10.1126/sageke.2006.6.re1

Tokuda, T., Chambers, J.K., Nakayama, H., Tatebe, H., Takahashi, E., Uchida, K., Ishii, R., Tomiyama, T., Une, Y., 2015. The domestic cat as a natural animal model of Alzheimer's disease. Acta Neuropathol. Commun. 3, 1–14. https://doi.org/10.1186/s40478-015-0258-3

Walker, L., McAleese, K.E., Johnson, M., Khundakar, A.A., Erskine, D., Thomas, A.J., McKeith, I.G., Attems, J., 2017. Quantitative neuropathology: an update on automated methodologies and implications for large scale cohorts. J. Neural Transm. 124, 671–683. https://doi.org/10.1007/s00702-017-1702-2

Waragai, M., Ho, G., Takamatsu, Y., Sekiyama, K., Sugama, S., Takenouchi, T., Masliah, E., Hashimoto, M., 2017. Importance of adiponectin activity in the pathogenesis of Alzheimer's disease. Ann. Clin. Transl. Neurol. 4, 591–600. https://doi.org/10.1002/acn3.436

Ward, R.J., Zucca, F.A., Duyn, J.H., Crichton, R.R., Zecca, L., 2014. The role of iron in brain ageing and neurodegenerative disorders. Lancet Neurol. https://doi.org/10.1016/S1474-4422(14)70117-6

Wilson, L.A., Heraty, L., Ashford, B.A., Coelho, S., Frangi, A.F., Pozo, J.M., Ince, P.G., Highley, J.R., 2021. Tissue Microarray (TMA) Use in Post Mortem Neuropathology. J. Neurosci. Methods 347, 108963. https://doi.org/10.1016/j.jneumeth.2020.108963

Wojtunik-Kulesza, K., Oniszczuk, A., Waksmundzka-Hajnos, M., 2019. An attempt to elucidate the role of iron and zinc ions in development of Alzheimer's and Parkinson's diseases. Biomed. Pharmacother. 111, 1277–1289. https://doi.org/10.1016/j.biopha.2018.12.140

Youssef, S.A., Capucchio, M.T., Rofina, J.E., Chambers, J.K., Uchida, K., Nakayama, H., Head, E., 2016. Pathology of the Aging Brain in Domestic and Laboratory Animals, and Animal Models of Human Neurodegenerative Diseases. Vet. Pathol. 53, 327–348. https://doi.org/10.1177/0300985815623997